International Journal of Nanoelectronics and Materials
IJNeaM
ISSN 1985-5761 | E-ISSN 2232-1535

Mechanochemical synthesis of Mg doped ZnO/CuO heterojunction composite-based electrode for electrochemical sensing

Marina Marzuki [a] *, Nurafzarini Mohd Rusdi [a], Ng Yik Hung [a], Nooraizedfiza Zainon [b], Mohd Zamzuri Mohammad Zain [a], and Zuraihana Bachok [b]

[a]*Faculty of Mechanical Engineering Technology, Universiti Malaysia Perlis, 02600 Arau, Perlis, Malaysia*
[b]*School of Mechanical Engineering, Universiti Sains Malaysia, 14300 Nibong Tebal, Penang, Malaysia*
** Corresponding author. e-mail: marina@unimap.edu.my*

Received 13 June 2024, Revised 19 September 2024, Accepted 27 December 2024

ABSTRACT

The influence of Mg doping and the impact of heterointerface growth mechanism of mechanochemically synthesized Mg-doped ZnO/CuO (MZC) heterojunction composite as electrode material for electrochemical sensing applications have been investigated. Thin-film composite electrode composed of bulk MZC nanocomposite deposited on ITO glass substrates using spin coating were fabricated. Structural analysis revealed that the hexagonal wurzite features of ZnO was preserved with Mg doping, and no new phases were developed. The MZC composite consists of prominent wurzite ZnO peaks along with peaks correspond to cubic monoclinic CuO. This finding agrees with the field emission scanning electron microscopy (FESEM) morphologies of ultra-small interconnected MZ and CuO particles that were reduced and had high defect levels due to the mechanochemical effect. Energy-dispersive X-ray spectroscopy (EDX) analysis confirmed the complete transformation of the starting materials. X-ray photoelectron spectroscopy (XPS) analysis confirmed the existence of ZnO and CuO compositions, as well as a Mg phase in the composite. Cyclic voltammetry analysis revealed an improved peak current and narrower anodic-cathodic potential separation from 233 μA of basic ZnO (Z) electrode to 245 μA on the Mg-doped ZnO/CuO composite electrodes (MZC) indicating higher sensitivity and a much higher charge transfer rate, respectively. The findings provide promising insights into Mg-doped ZnO/CuO bulk heterojunction nanocomposite systems and their potential for electrochemical sensing applications.

Keywords: *ZnO, CuO, Mechanochemical synthesis, Cyclic voltammetry*

1. INTRODUCTION

Biosensors play a vital role in detecting and monitoring diseases in the healthcare sector. Currently, glucose sensors account for approximately 75% of the biosensors industry, as they directly correlate with the health consequences of diabetes, which affects nearly 382 million people worldwide [1]. Therefore, there is a pressing need for early detection and control of diabetes. However, most sensor types require glucose oxidase (GOx) as a reducing/oxidizing mediator. Although GOx-based sensors offer high, reliable sensitivity, and rapid responsiveness [2], they have some limitations, including instability, shorter lifespans, relatively high costs, and complicated preparation procedures. Nevertheless, there is still a significant scope for improving the affordability and reliability of glucose sensors. Enzyme-free sensors are seen as suitable alternatives for daily glucose monitoring, as they are easier to prepare, less costly, have high stability, and offer real-time monitoring and repeatability [3, 4]. The properties of nanostructured materials are highly dependent on their morphology (attributes and size). Therefore, controlling these parameters would result in changes in optical and electrical properties. Doping is an effective method for tuning semiconductor properties such as polarity, bandgap, crystallinity as well as electrical conductivity. Due to its non-toxic, electrochemical stability and cost-effective material, nanoscale ZnO structure has emerged as a promising material for electrochemical biosensing. Among transitional metal doping elements, Mg can be considered as potential dopant in ZnO nanostructures due to its relatively high solubility. Mg is recognized to significantly improve ZnO gas sensing performance, enhance photocatalytic activities [5, 6], improve optical properties. In addition, several reports on metal oxides heterostructures have demonstrated that coupling of different nanostructured semiconductors have augmented the performance by improved current confinement compared to a homojunction device [7] and by mutual separation/transfer of charge carriers through the junction interfaces, as it slows down the recombination rate [8]. Electrochemical reactions are strongly influenced by the characteristics of the electrode surfaces. A high surface-to-volume ratio of the active sensing surface enhances sensitivity. Our study demonstrates the potential of Mg:ZnO/CuO heterojunction composite electrodes in electrochemical sensing applications. We utilized the mechanochemical synthesis achieved through ball milling process to reduce the particle size and increase the effective surface contact area. This method produced a bulk heterojunction composite that increases the effective contact between n-Mg:ZnO and p-CuO. Its performance can

be attributed to the electroactive properties of ZnO and CuO and the large surface area provided by the composite nanostructures.

2. EXPERIMENTAL PROCEDURES

2.1. Materials

$Zn.CH_3(COOH)_2$ (Sigma Aldrich), as-received CuO nanoparticles (99.9% purity, Merck) were used as the precursors, MgCl (Kanto Chemical) was used as the doping source, C_2H_7NO (Sigma Aldrich), NaOH and C_3H_8O (Merck) were used as stabilizer, catalyst and solvent; respectively. Deionized water was used on necessary stages of the experiment. CH_3COOH and Triton X-100 (Sigma Aldrich) surfactant were mixed with the synthesized Mg doped ZnO (MZ) and CuO nanoparticles to form slurry. All chemicals and solvent used in this synthesis are reagent grade. Indium tin oxide (ITO) glass substrates with thickness of 0.5 mm were used as thin film template for all specimens. The synthesis of ZnO (Z) and Mg doped ZnO (MZ) has been detailed in our earlier report [9].

2.2. Solid-state Mechanochemical Synthesis of ZC and MZC Heterojunction Nanocomposites

Baseline ZnO (Z) was prepared by sol-gel synthesis. 0.1M of Zn2+ sol-gel was prepared by dissolving $(CH_3COO)_2Zn.2H_2O$ in C_3H_8O solvent by vigorous stirring at 600 rpm and temperature 50°C for 60 minutes. 1 M NaOH solution is titrated into the solution until pH9 is reached. Subsequently, an equimolar concentration of C_2H_7NO was added dropwise. At this stage, a homogenous and clear solution is obtained. The stirring was continued for 30 minutes; and the prepared solution was allowed to cool down to room temperature for 24 hours to allow complete condensation and sol-gel formation. Subsequently, the solution was centrifugated at 3000 rpm for 30 minutes to speed up the isolation of the condensed sol-gel from solvent. The resulting sol-gel was dried at 100˚C for 60 minutes then manually ground to obtain white ZnO precipitates. For Mg-doped ZnO (MZ) nanoparticles, the same step of preparing baseline Z was applied. During the solution preparation, 0.05M MgcCl was added into the solution. Mg:ZnO/CuO (MZC) heterojunction composites was procured by mechanochemical reactions via HEBM method of the synthesized MZ particles and as-purchased CuO (99% purity, FW: 79.54 g/mol, Merck). An equal molarity of the two compounds with a ratio of 1:1 was measured. The powders are mixed by planetary ball mill (Pulverisette P6 ball mill, 300 rpm, stainless steel ball) to provide mechanochemical reactions to achieve homogeneity and to increase surface contact area-to-volume ratio. The total milling time is 2 hours. Due to the machine limitations, the milling process is repeated several times with each cycle for 10 minutes and rest for 10 minutes. Subsequently, the milled compound was ground in a mortar at room temperature with added 0.035 M CH3COOH and Triton X-100 suspension drop by drop to form a thick slurry and deposited as thin films on ITO substrates. The films were annealed at 500˚C for an hour.

2.3. Properties Characterization

The phase evaluation and crystallographic study of the synthesized thin films were performed with X-ray-Diffraction (XRD) (Bruker, Germany). Surface morphology of the specimens was observed with Field Emission Scanning Electron Microscopy (FESEM) (ZEISS GeminiSEM 360). The optical properties of the specimens were analyzed by Ultraviolet-Visible (UV-Vis) spectroscopy (Perkin Elmer Lambda 35, USA) between 200–800 nm wavelength.

2.4. Electrochemical Response Study

To investigate the applicability of such heterointerface nanocomposite as electrode material, electrochemical test towards oxidation-reduction (redox) conversion of ferricyanide ($Fe(CN)_6$) was conducted. The redox effect on peak current of 1 mmol/L $Fe(CN)_6$ redox electrolyte has been carried out by cyclic voltammetry (CV) method [8]. To perform the CV study, conventional three electrode system was set up on potentiostat (Metrohm Autolab, USA). The CV activity was real-time observed at start potential of 0 V as reference with potential window of –1 to 1 V, lower vortex potential of –1, stop potential at 0, number of scans per cycle of 6, scan rate of 0.1 V/s and scan step of 0.00244 V at room temperature.

3. RESULTS AND DISCUSSION

3.1. Physical Properties

XRD analysis was performed to observe the Mg doping effect onto ZnO host structure and shown in Figure 1. From the Mg-doped ZnO (MZ) diffraction pattern, the ZnO phases denoted by the (100), (002), (101) and (103) diffraction peaks were consistent with the ZnO (Z) specimen which signifies that the MZ specimens are a constituent of pristine ZnO [10]. The MZC peak profile shows the co-existence of ZnO and CuO in the composite system. In the zoom in

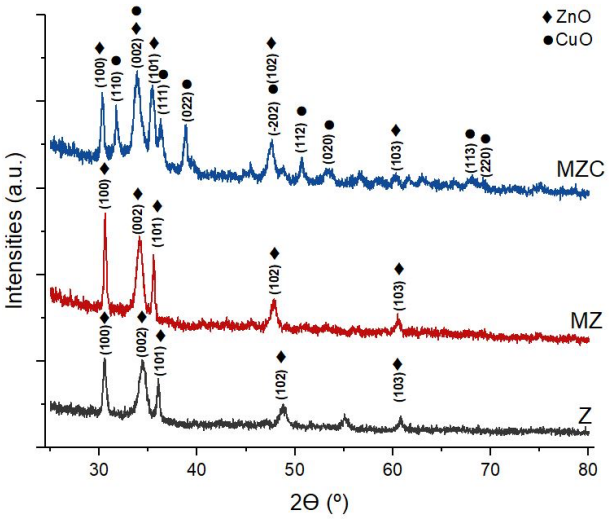

Figure 1. XRD spectra of the thin films

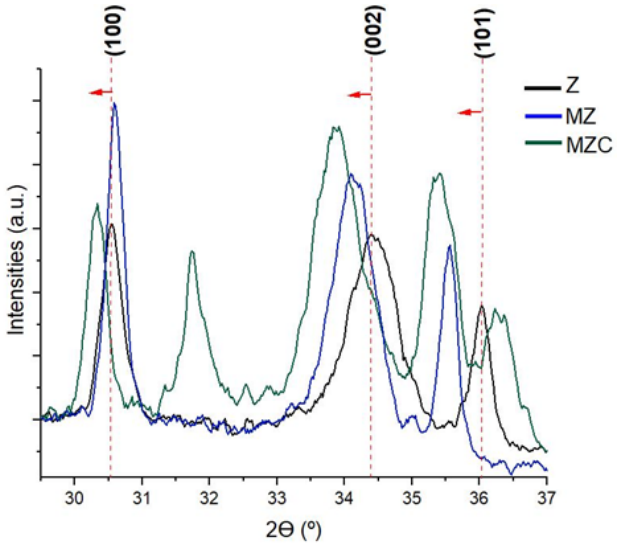

Figure 2. XRD spectra zoom-in of the ZnO preferred growth peaks

spectra of ZnO preferred peaks (Figure 2), the plots show a peak shift towards lower diffraction angle (2θ). Residual stress might shift some peaks in one direction which is likely due to the need to balance stress at grain boundaries and satisfy the constraints on the strain tensor in the crystal lattice [11]. For instance, a tensile stress along one direction must be balanced by a compressive stress in the normal direction, hence the direction of peak shift is often *hkl* dependent. The shifting also indicates the occurrence of lattice strain defect [12] in the film caused by the substitution of smaller ionic radii Mg (0.57 Å) into ZnO's lattice (0.60 Å) that allows stress relief. A raised $(100)_{ZnO}$ peak is seen in MZ spectra and peak broadening in other ZnO main peaks indicating a crystal reordering via annealing [13]. The same peak shift trend was also observed in MZC specimen (blue line).

The morphological observations of the samples were carried by FESEM (Figure 3). Physically all film specimens are observed to have a compact and continuous distribution. As seen in the high magnification images, all ZnO-based films (Z and MZ) are composed of nanograins, where the grain size increases seen on the MZ specimen (Figure 3(b)). The growth of solid nanocrystals in solution is due to the self-selective nucleation [14]. When ZnO is doped, lattice distortion occurred owing to Mg and Zn size difference that results in stress development in different directions. Subsequently, the developed stress broke and fractured the particles bonding. The formed nanostructures then became a bridge for conversion of small crystals to aggregated crystals that plays the primary role in the nano surfaces' changes. In addition, the expansion of lattice volumes that led to the overall increase of crystal size may be due to the Mg atoms' interstitial entrance in ZnO lattice. As estimated in the structural analysis, ultra-small particles were seen because of MZC specimen (Figure 3(c)). High-energy ball milling is not merely a physical size reduction process like conventional grinding; it also induces mechanochemical reactions at the nanoscale during milling. These reactions initiate composite formation at the

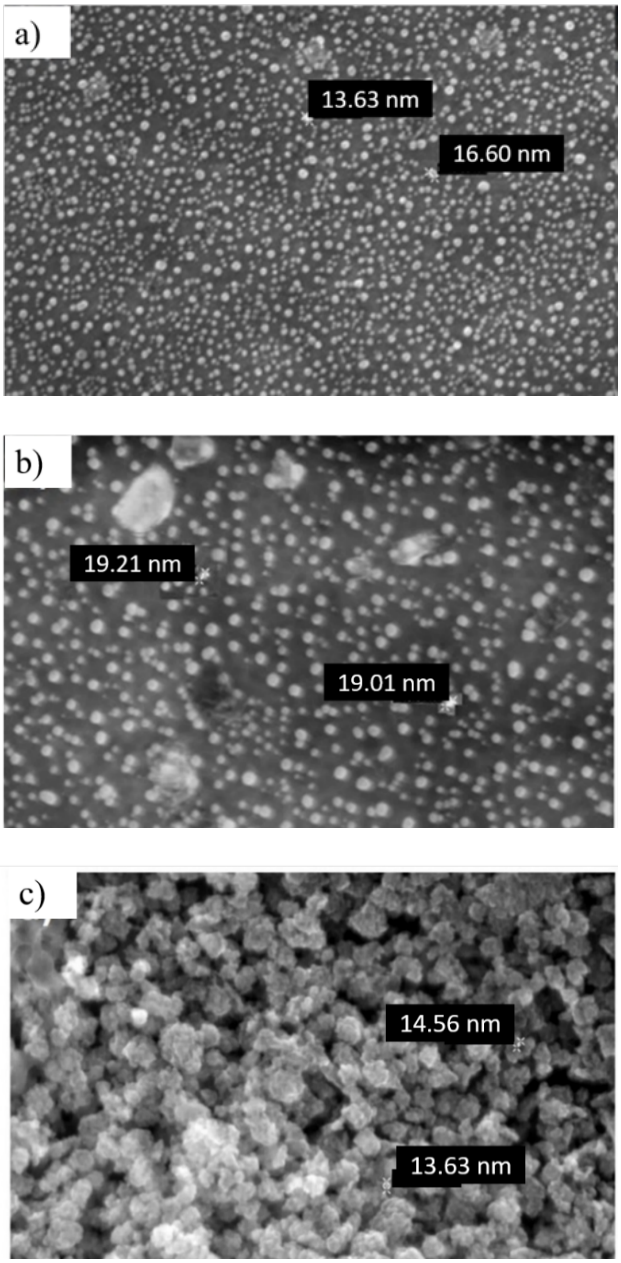

Figure 3. (a) ZnO nanoparticles (Z); (b) Mg-doped ZnO nanoparticles (MZ), and (c) Mg-doped ZnO/CuO (MZC) nanocomposite

interfaces of regenerating nanograins, which continuously provide fresh surfaces for interfacial interactions. Consequently, chemical reactions that typically require high temperatures occur at low temperatures within the ball mill, eliminating the need for external heating [15]. This solid-state displacement reaction leads to a finer mixture of product phases compared to the original matrix, aligning with previous studies that employed similar materials and methods [16]. The resulting ultra-fine mixture of ZnO and CuO in the MZC specimen achieves a higher aspect ratio.

XPS analysis was conducted to reveal the surface composition and chemical states of the synthesized MZC nanocomposite thin film. Calibration of the estimated energy bands was referred to the adsorbed C 1s peak. The observed peaks confirmed the existence of Mg, ZnO and CuO

compounds. Asymmetric peaks at 1044.25 eV and 1021.25 eV correspond to Zn $2p_{½}$ and Zn $2p_{3/2}$ were seen (Figure 4(a)). This set of binding energies may be evidence for the Zn2+ oxidation state [15–17]. The Zn peak was positioned at lower binding energy compared to of standard bulk ZnO's [20], that could be associated with the formation of other Zn-based components during the synthesis stage. A fraction of the ZnO nanostructures has weakened Zn–O bonding energy brought about the formation of new compounds that could be either in metallic or interstitial states [21]. At the same time, the weakened state allowed Mg substitution in the ZnO matrix. Figure 4(b) shows the Mg 1s peak 1. together with peaks correspond to the Mg oxide phase (MgO) at 1306.08 eV and metallic Mg (1304.18 eV) [22] . Figure 4(c) shows the distinctive Cu^{2+} peaks at 933.37 eV corresponds to $Cu2p_{3/2}$ and 951.58 eV corresponds to $Cu2p_{1/2}$ peaks. The binding energies correspond to the bivalent state of Cu^{2+}. A satellite peak noted at 940.1 eV that is attributed to a partially filled $3d^9$ block of Cu^+ [23]. The observed valence state and satellite peak strongly suggest that Cu has been oxidized to CuO [16, 22].

3.2. Electrode Characteristics of the Composites

To assess the potential of this p-n interface nanocomposite as an electrode material, we conducted an electrochemical test to measure the redox conversion of ferricyanide $(Fe(CN)_6$. The curve of all specimen electrodes showed a pair well-defined quasi-reversible peaks along with important characteristics of capacitive current, Faradaic current, oxidation and reduction peaks (Figure 5) which indicates the establishment of the study [23–25]. Anodic peak analysis revealed significantly higher redox activity on MZ and MZC electrodes (245 μA) compared to the baseline Z electrode (233 μA). The enhanced performance of MZ and MZC electrodes can be attributed to the formation of a metal-semiconductor Schottky contact [15], facilitating charge carrier transfer across the ZnO conduction band and oxide nanocomposite/electrolyte interface [28]. For MZC composite electrodes, the anodic peak resulted from the oxidation of Cu(I) to Cu(II), while cathodic peaks corresponded to the reduction of Cu(II) back to Cu(I) [29]. The heterointerface promoted higher electrical conductivity, faster electron transfer kinetics, and a larger electroactive surface area, leading to improved electrochemical response. Cu's inherent electrical conductivity at low overpotential also contributed to the enhancement. The synergistic effect between Mg:ZnO and CuO at the heterointerface facilitated electron transfer between the redox electrolyte and the MZC electrode surface. The narrower potential separation (ΔEp) between anodic and cathodic peaks for MZ and MZC (688.43 mV and 834.96 mV, respectively) compared to the baseline Z electrode (864.33 mV) indicates a faster charge transfer rate [30], demonstrating the effectiveness of doping and hetero-coupling.

Anodic peak analysis revealed significantly higher redox activity on MZ and MZC electrodes (245 μA) compared to the baseline Z electrode (233 μA). The enhanced performance of MZ and MZC electrodes can be attributed to

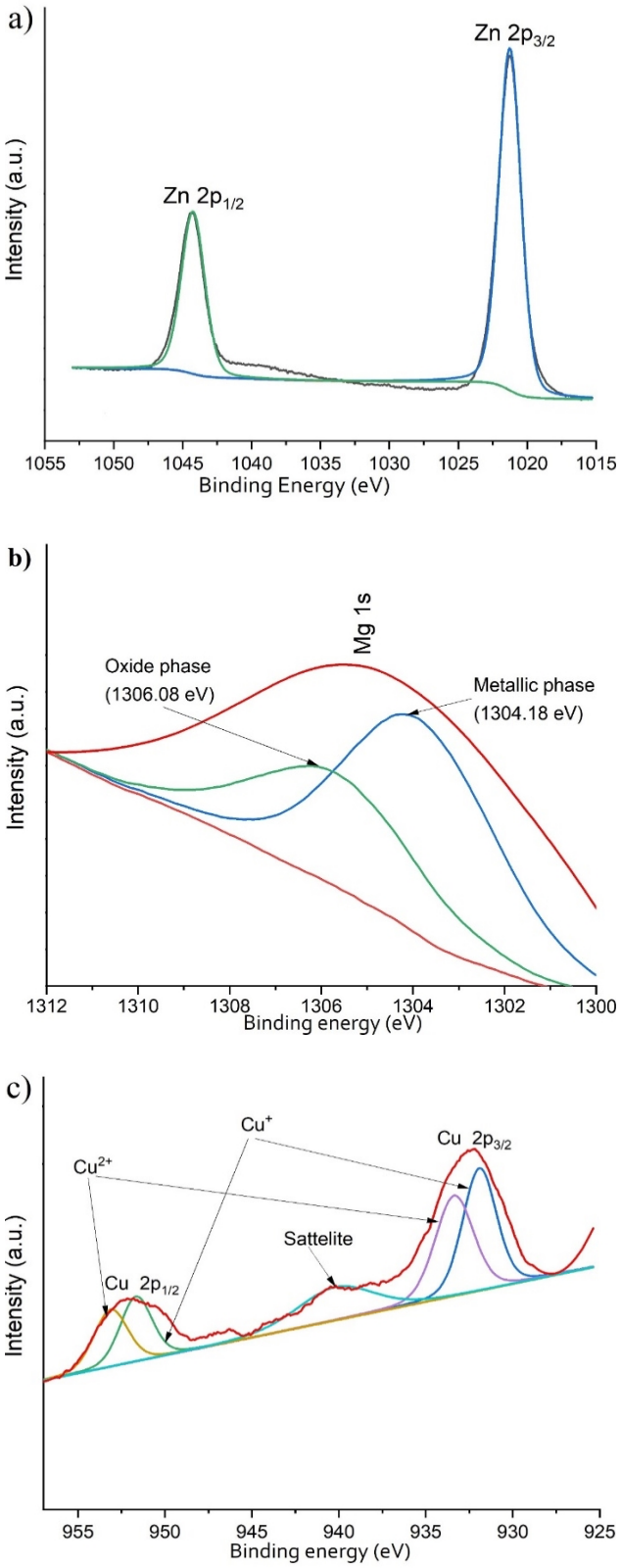

Figure 4. XPS spectra of the MZC composite thin film; (a) Zn peaks, (b) Mg peaks and (c) Cu peaks

the formation of a metal-semiconductor Schottky contact [15], facilitating charge carrier transfer across the ZnO conduction band and oxide nanocomposite/electrolyte interface [28]. For MZC composite electrodes, the anodic peak resulted from the oxidation of Cu(I) to Cu(II), while cathodic peaks corresponded to the reduction of Cu(II) back

to Cu(I) [29]. The heterointerface promoted higherelectrical conductivity, faster electron transfer kinetics, and a larger electroactive surface area, leading to improved electrochemical response. Cu's inherent electrical conductivity at low overpotential also contributed to the enhancement. The synergistic effect between Mg:ZnO and CuO at the heterointerface facilitated electron transfer between the redox electrolyte and the MZC electrode surface. The narrower potential separation (ΔEp) between anodic and cathodic peaks for MZ and MZC (688.43 mV and 834.96 mV, respectively) compared to the baseline Z electrode (864.33 mV) indicates a faster charge transfer rate [30], demonstrating the effectiveness of doping and hetero-coupling.

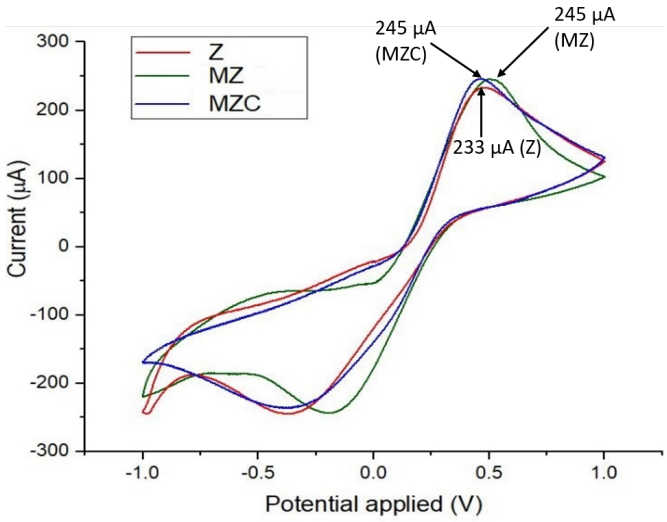

Figure 5. Cyclic voltammogram of the electrodes

4. CONCLUSION

This study investigates the properties of Mg-doped ZnO and Mg:ZnO/CuO bulk heterojunction nanocomposites synthesized using mechanochemical synthesis. Structural analysis confirms the successful incorporation of Mg into ZnO and the hetero coupling with CuO. Compositional analysis confirms the complete transformation of the precursors into Mg-doped ZnO and Mg:ZnO/CuO composites. Cyclic voltammetry (CV) analysis of the electrode specimens reveals that MZ and MZC electrodes exhibit better electrocatalytic activity and stable responses than baseline ZnO (Z). The structure of the electrode surface contributes to the CV properties and is crucial for estimating the mass of transferred electrons. This work may provide a useful insight into a simpler way to synthesize Mg:ZnO/CuO nanocomposites with tailored Mg doping levels and high heterointerfaces, which have the potential to be applied in biosensing devices.

ACKNOWLEDGMENTS

The authors would like to acknowledge the support from the Fundamental Research Grant Scheme (FRGS) under a grant number of FRGS/1/2019/TK03/UNIMAP/02/23 from the Ministry of Education Malaysia.

REFERENCES

[1] Y. Huang, J. Xu, J. Liu, X. Wang, and B. Chen, "Disease-Related Detection with Electrochemical Biosensors: A Review," *Sensors*, vol. 17, no. 10, p. 2375, Oct. 2017, doi: 10.3390/s17102375.

[2] X. Wang, S. Li, L. Xie, X. Li, D. Lin, and Z. Zhu, "Low-temperature and highly sensitivity H_2S gas sensor based on ZnO/CuO composite derived from bimetal metal-organic frameworks," *Ceramics International*, vol. 46, no. 10, pp. 15858–15866, Jul. 2020, doi: 10.1016/j.ceramint.2020.03.133.

[3] Z. Haghparas, Z. Kordrostami, M. Sorouri, M. Rajabzadeh, and R. Khalifeh, "Highly sensitive non-enzymatic electrochemical glucose sensor based on dumbbell-shaped double-shelled hollow nanoporous CuO/ZnO microstructures," *Scientific Reports*, vol. 11, no. 1, p. 344, Jan. 2021, doi: 10.1038/s41598-020-79460-2.

[4] W. K. Khalef, A. A. Aljubour, and A. D. Faisal, "Glucose biosensor electrode fabrication based on CuO /ZnO nanostructures," *Journal of Physics: Conference Series*, vol. 1795, no. 1, p. 012038, Mar. 2021, doi: 10.1088/1742-6596/1795/1/012038.

[5] A. Elhalil *et al.*, "Photocatalytic degradation of caffeine as a model pharmaceutical pollutant on Mg doped ZnO-Al_2O_3 heterostructure," *Environmental Nanotechnology, Monitoring & Management*, vol. 10, pp. 63–72, Dec. 2018, doi: 10.1016/j.enmm.2018.02.002.

[6] R. Yousefi, J. Beheshtian, S. M. Seyed-Talebi, H. R. Azimi, and F. Jamali-Sheini, "Experimental and Theoretical Study of Enhanced Photocatalytic Activity of Mg-Doped ZnO NPs and ZnO/rGO Nanocomposites," *Chemistry – An Asian Journal*, vol. 13, no. 2, pp. 194–203, Jan. 2018, doi: 10.1002/asia.201701423.

[7] S. Annathurai, S. Chidambaram, B. Baskaran, and G. K. D. Prasanna Venkatesan, "Green Synthesis and Electrical Properties of p-CuO/n-ZnO Heterojunction Diodes," *Journal of Inorganic and Organometallic Polymers and Materials*, vol. 29, no. 2, pp. 535–540, Mar. 2019, doi: 10.1007/s10904-018-1026-1.

[8] B. Li and Y. Wang, "Facile synthesis and photocatalytic activity of ZnO–CuO nanocomposite," *Superlattices and Microstructures*, vol. 47, no. 5, pp. 615–623, May 2010, doi: 10.1016/j.spmi.2010.02.005.

[9] M. Marzuki, N. Mohd. Rusdi, M. Z. M. Zain, and M. Izaki, "Multi-staged sol–gel synthesis of Mg doped ZnO/CuO core-shell heterojunction nanocomposite: dopant induced and interface growth response," *Journal of Sol-Gel Science and Technology*, vol. 100, no. 3, pp. 388–403, Dec. 2021, doi: 10.1007/s10971-021-05679-8.

[10] Muhammad Asnawir Nasution *et al.*, "The Enhancement Light Absorption of ZnO-TiO_2 Nanocomposite as Photoanode," *International Journal of Nanoelectronics and Materials (IJNeaM)*, vol. 16, no. 4, pp. 883–890, Oct. 2024, doi: 10.58915/ijneam.v16i3.1374.

[11] A. Bahadur, B. R. Kumar, A. S. Kumar, G. G. Sarkar, and J. S. Rao, "Development and comparison of residual stress measurement on welds by various methods," *Materials Science and Technology*, vol. 20, no. 2, pp. 261–269, Feb. 2004, doi: 10.1179/026708304225012332.

[12] M. Marzuki, M. Z. M. Zain, W. A. R. A. Wan Ibrahim, N. Zainon, and R. N. Ahmad, "Doping content dependencies on the structure modification and bandgap broadening of Al induced sol-gel derived ZnO nanostructures," *International Journal of Nanoelectronics and Materials*, vol. 14, no. 4, pp. 373–388, 2021.

[13] J. Ye *et al.*, "The growth and annealing of single crystalline ZnO films by low-pressure MOCVD," *Journal of Crystal Growth*, vol. 243, no. 1, pp. 151–156, Aug. 2002, doi: 10.1016/S0022-0248(02)01474-4.

[14] M. Shirvani and L. Naji, "Effect of Seed Layer on the Morphology of Zinc Oxide Nanorods as an Electron Transport Layer in Polymer Solar Cells ," *International Journal of Nanoscience and Nanotechnology*, vol. 16, no. 3, pp. 201–208, 2020.

[15] B. A. Albiss, H. S. Abdullah, and A. M. Alsaad, "Structural and Electrical Properties of Glucose Biosensors Based on ZnO and ZnO-CuO Nanostructures," *Current Nanoscience*, vol. 18, no. 2, pp. 255–265, Mar. 2022, doi: 10.2174/1573413717666210301111000.

[16] D. A. Wilson, K. Gurung, and M. A. Langell, "Effect of zinc substitution on the growth morphology of ZnO-CuO tenorite solid solutions," *Journal of Crystal Growth*, vol. 562, p. 126062, May 2021, doi: 10.1016/j.jcrysgro.2021.126062.

[17] A. B. Appiagyei and J. I. Han, "Potentiometric Performance of a Highly Flexible-Shaped Trifunctional Sensor Based on ZnO/V_2O_5 Microrods," *Sensors*, vol. 21, no. 7, p. 2559, Apr. 2021, doi: 10.3390/s21072559.

[18] M. A. Khan, Y. Wahab, R. Muhammad, M. Tahir, and S. Sakrani, "Catalyst-free fabrication of novel ZnO/CuO core-Shell nanowires heterojunction: Controlled growth, structural and optoelectronic properties," *Applied Surface Science*, vol. 435, pp. 718–732, Mar. 2018, doi: 10.1016/j.apsusc.2017.11.071.

[19] A. Awais *et al.*, "Facial synthesis of highly efficient non-enzymatic glucose sensor based on vertically aligned Au-ZnO NRs," *Journal of Electroanalytical Chemistry*, vol. 895, p. 115424, Aug. 2021, doi: 10.1016/j.jelechem.2021.115424.

[20] J. Das *et al.*, "Micro-Raman and XPS studies of pure ZnO ceramics," *Physica B: Condensed Matter*, vol. 405, no. 10, pp. 2492–2497, May 2010, doi: 10.1016/j.physb.2010.03.020.

[21] J. Afonso, R. Leturcq, P. L. Popa, and D. Lenoble, "Transparent p-$Cu_{0.66}Cr_{1.33}O_2$/n-ZnO heterojunction prepared in a five-step scalable process," *Journal of Materials Science: Materials in Electronics*, vol. 30, no. 2, pp. 1760–1766, Jan. 2019, doi: 10.1007/s10854-018-0448-4.

[22] C. Fu Lin, C. Haur Kao, C. Yu Lin, Y. Wen Liu, and C. Hsiang Wang, "The electrical and physical characteristics of Mg-doped ZnO sensing membrane in EIS (electrolyte–insulator–semiconductor) for glucose sensing applications," *Results in Physics*, vol. 16, p. 102976, Mar. 2020, doi: 10.1016/j.rinp.2020.102976.

[23] R. Sahay, J. Sundaramurthy, P. Suresh Kumar, V. Thavasi, S. G. Mhaisalkar, and S. Ramakrishna, "Synthesis and characterization of CuO nanofibers, and investigation for its suitability as blocking layer in ZnO NPs based dye sensitized solar cell and as photocatalyst in organic dye degradation," *Journal of Solid State Chemistry*, vol. 186, pp. 261–267, Feb. 2012, doi: 10.1016/j.jssc.2011.12.013.

[24] V. Kumari, S. Yadav, J. Jindal, S. Sharma, K. Kumari, and N. Kumar, "Synthesis and characterization of heterogeneous ZnO/CuO hierarchical nanostructures for photocatalytic degradation of organic pollutant," *Advanced Powder Technology*, vol. 31, no. 7, pp. 2658–2668, Jul. 2020, doi: 10.1016/j.apt.2020.04.033.

[25] S. Chabri, A. Dhara, B. Show, D. Adak, A. Sinha, and N. Mukherjee, "Mesoporous CuO–ZnO p–n heterojunction based nanocomposites with high specific surface area for enhanced photocatalysis and electrochemical sensing," *Catalysis Science & Technology*, vol. 6, no. 9, pp. 3238–3252, 2016, doi: 10.1039/C5CY01573A.

[26] M. G. Peleyeju, "Electrochemical and solar photoelectrocatalytic oxidation of selected organic compounds at carbon-semiconductor based electrodes," 2017.

[27] A. Sulciute *et al.*, "ZnO Nanostructures Application in Electrochemistry: Influence of Morphology," *The Journal of Physical Chemistry C*, vol. 125, no. 2, pp. 1472–1482, Jan. 2021, doi: 10.1021/acs.jpcc.0c08459.

[28] A. Mahmoud *et al.*, "Cu-Doped ZnO Nanoparticles for Non-Enzymatic Glucose Sensing," *Molecules*, vol. 26, no. 4, p. 929, Feb. 2021, doi: 10.3390/molecules26040929.

[29] J. Wu and F. Yin, "Easy Fabrication of a Sensitive Non-Enzymatic Glucose Sensor Based on Electrospinning CuO-ZnO Nanocomposites," *Integrated Ferroelectrics*, vol. 147, no. 1, pp. 47–58, Jan. 2013, doi: 10.1080/10584587.2013.790695.

[30] X. Dong *et al.*, "Hybrid structure of zinc oxide nanorods and three dimensional graphene foam for supercapacitor and electrochemical sensor applications," *RSC Advances*, vol. 2, no. 10, p. 4364, 2012, doi: 10.1039/c2ra01295b.